ORIGINAL ARTICLE

Radiological characteristics of skeletal growth in neonates and infants with achondroplasia

Daisuke Miyahara ( )[1,2], Kosei Hasegawa (haseyan@md.okayama-u.ac.jp)[3], Yuko Ago ( )[3], Natsuko Futagawa ( )[1,3], Hiroyuki Miyahara ( )[1], Yousuke Higuchi ( )[3], Kazuki Yamada ( )[4], Tomonori Tetsunaga ( )[4], Tadashi Moriwake ( )[5], Hiroyuki Tanaka ( )[6], and Hirokazu Tsukahara ( )[1]

[1]Department of Pediatrics, Okayama University Graduate School of Medicine, Dentistry and Pharmaceutical Sciences, 2-5-1 Shikata-cho, Kita-ku, Okayama 700-8558, Japan

[2]Department of Pediatrics, Hiroshima City Hiroshima Citizens Hospital, 7-33 Motomachi, Naka-ku, Hiroshima 730-8518, Japan

[3]Department of Pediatrics, Okayama University Hospital, 2-5-1 Shikata-cho, Kita-ku, Okayama 700-8558, Japan

[4]Department of Orthopedics, Okayama University Hospital, 2-5-1 Shikata-cho, Kita-ku, Okayama 700-8558, Japan

[5]Department of Pediatrics, Iwakuni Clinical Center, National Hospital Organization, 1-1-1 Atagomachi, Iwakuni 740-0037, Japan

[6]Department of Pediatrics, Okayama Saiseikai General Hospital, 1-7-18 Ifuku-cho, Kita-ku, Okayama 700-8511, Japan

Correspondence

Kosei Hasegawa, M.D., Ph.D., Department of Pediatrics, Okayama University Hospital, 2-5-1 Shikata-cho, Kita-ku, Okayama 700-8558, Japan. Tel.: +81-86-235-7249; Fax: +81-86-221-4745; E-mail: haseyan@md.okayama-u.ac.jp.

Author contributions: Daisuke Miyahara: Study design, clinical data collection, measurement of bone parameters, genetic analysis, writing – original draft, and writing – review and editing. Kosei Hasegawa: Study design, clinical data collection, measurement of bone parameters, genetic analysis, and writing – review and editing. Yuko Ago: Clinical data collection and genetic analyses. Natsuko Futagawa: Clinical data collection and genetic analysis. Hiroyuki Miyahara: Study design and clinical data collection. Yousuke Higuchi: Clinical data collection and genetic analyses. Kazuki Yamada: Clinical data collection. Tomonori Tetsunaga: Clinical data collection. Tadashi Moriwake: Study design and clinical data

collection. Hiroyuki Tanaka: Study design, clinical data collection, and manuscript review. Hirokazu Tsukahara: Manuscript review. All authors have read and approved the final manuscript.

Conflict of interests: Hiroyuki Tanaka received honoraria for lecture fees from KYOWA KIRIN Co., Ltd. No other authors have any financial support or relationships that may pose a conflict of interest.

Funding information: This study was supported by a Grant-in-Aid for Research from the Foundation for Growth Science, a Grant-in-Aid for Health Labor Sciences Research (No. 200936241A and 201324078 B) from the Ministry of Health, Labor and Welfare of Japan, and a Grant-in-Aid for Practical Research Project for Rare/Intractable Diseases (No. 16ek0109135h0002) from the Japan Agency for Medical Research and Development.

Ethics approval statement: The genetic study and analysis of radiographs of patients with achondroplasia were approved by the Ethics Committee of Okayama University Hospital (approval no.: 1701-038).

Patient consent statement: Written informed consent was obtained from the guardians of patients.

Data availability statement: All the measurement data are available in Supplemental Tables 1 and 2.

Acknowledgements: The authors thank all patients for their participation in this study.

Abstract

Achondroplasia (ACH) is the most common form of skeletal dysplasia characterized by a rhizomelic short stature. Radiological skeletal findings in pediatric and adult patients with ACH include short long bones, a relatively longer fibula compared to the tibia, a narrow lumbar interpedicular distance, and a hypoplastic iliac wing. Nonetheless, the characteristics of skeletal growth during the neonatal and infantile periods have scarcely been explored. Therefore, this retrospective study aimed to analyze the radiological skeletal growth during the neonatal and infantile periods in 41 Japanese patients with genetically confirmed ACH. The length of long bones in the upper and lower limbs and the lumbar interpedicular distances at L1 and L4 were measured. These parameters showed significant positive correlations with age. The upper segment-to-lower segment ratio in the lower limbs resembled the data of healthy controls from previous reports. The L1/L4 and fibula/tibia ratios increased with age, suggesting that some representative skeletal phenotypes of ACH were less distinct during the neonatal and infantile periods. In conclusion, for the first time, this study radiologically characterized skeletal growth during the neonatal and infantile periods of patients with genetically confirmed ACH.

KEYWORDS

bone development, dwarfism, growth, infant, radiography

1 | INTRODUCTION

Achondroplasia (ACH) is the most common form of skeletal dysplasia characterized by a rhizomelic short stature. The short stature in ACH mainly results from the shortening of long bones in the lower limbs. The heterozygous p.Gly380Arg variant of fibroblast growth factor receptor 3 (*FGFR3*), which exhibits constitutional activation, has been identified in more than 95% of patients with ACH (Hasegawa & Tanaka, 2014; Rousseau et al., 1994; Shiang et al., 1994). The constitutional activation of *FGFR3*, which is a suppressor of endochondral ossification, causes skeletal abnormalities and clinical symptoms due to abnormal endochondral ossification. Foramen magnum stenosis is common among patients with ACH, and spinal cord compression at the cervicomedullary junction can lead to complications such as sleep apnea, myelopathy, hydrocephalus, and sudden death (Ireland et al., 2014). The symptoms of spinal canal stenosis include pain in the extremities, numbness, muscle weakness, motor impairment, bladder and rectal dysfunction, and intermittent claudication, which are also frequently observed in adolescents and adults with ACH (Horton et al., 2007).

Previous studies have reported radiological bone parameters during skeletal development in children and adults with ACH and have confirmed some skeletal characteristics observed in ACH, such as narrowing of the interpedicular distance and a relatively long fibula (Langer et al., 1967; Matsui et al., 1998; Matsui et al., 2001; Nehme et al., 1976; Shelmerdine et al., 2016; Wynne-Davies et al., 1981). In contrast to children and adults, the skeletal characteristics during the neonatal and infantile periods have

scarcely been reported except for two studies (Langer et al., 1967; Shelmerdine et al., 2016). To the best of our knowledge, radiologically analyzed longitudinal skeletal growth during the neonatal and infantile periods in patients with genetically confirmed ACH has not been reported. This led us to the hypothesis that radiological bone parameters in patients with ACH may also exhibit distinct characteristics during the neonatal and infantile periods which are not observed from pediatric to adult patients.

The present study aimed to analyze the radiological characteristics of skeletal development during the neonatal and infantile periods in patients with ACH and heterozygous p.Gly380Arg variant of *FGFR3*.

2 | MATERIALS AND METHODS

2.1 | Editorial policies and ethical considerations

The genetic study and analysis of radiographs of patients with ACH were approved by the Ethics Committee of Okayama University Hospital (approval no.: 1701-038). This study was conducted in accordance with the ethical guidelines for medical and biological research involving human participants in Japan and with the 1964 Declaration of Helsinki and its later amendments, and written informed consent was obtained from the guardians of each patient to use the genetic testing results and radiographs for retrospective research.

2.2 | Study design and data collection

This multicenter, retrospective, observational study included 41 Japanese patients (23 males and 18 females) who were clinically diagnosed with ACH at the Okayama University Hospital, Iwakuni Clinical Center, and other hospitals in Japan. The dataset was a combination of cross-sectional and longitudinal data. Preterm children born before 37 weeks of gestational age, patients receiving growth hormone therapy or other growth-promoting treatments, and those with any chronic disease or comorbidities that could affect their growth were excluded.

Genetic analysis of *FGFR3* was conducted from 2008 to 2023 in the laboratory of the Department of Pediatrics at the Okayama University Hospital. Genomic DNA was extracted from the leukocytes of patients with ACH using the QIAamp DNA Blood Mini Kit (Qiagen Inc., Tokyo, Japan). All coding exons and exon-intron boundaries of *FGFR3* were examined using the standard polymerase chain reaction (PCR) method; the sequences of PCR primers used in this study are available upon request. The obtained PCR products were purified using the QIAquick PCR Purification Kit (Qiagen Inc.) and were sequenced using the BigDye Terminator v3.1 Cycle Sequencing Kit and ABI PRISM 310 Genetic Analyzer (Thermo Fisher Scientific Inc., Tokyo, Japan).

Anterior-to-posterior radiographs of bones taken from birth to 4 years of age for the purpose of diagnosis and clinical care were analyzed. All skeletal parameter measurements were performed on Digital

Imaging and Communications in Medicine (DICOM) radiographic data using OsiriX Lite (Pixmeo, Geneva). The following skeletal parameters were assessed, as shown in Figure 1: the lengths of the humerus (Hum), radius (Rad), ulna (Uln), femur (Fem), tibia (Tib), and fibula (Fib); and the interpedicular distances at the first (L1) and fourth (L4) lumbar vertebrae. For long bone measurements, we recorded the diaphyseal bone lengths, not the total bone lengths, because the epiphyses are unossified in early infancy. When radiographs were obtained from both sides, the length of the long bones was measured on the left side. When radiographs were obtained from the right side only, we measured on the right side. All measurements were performed by the first author, some of which were repeated by the corresponding author to prevent any measurement bias. Both observers were pediatricians with over 10 years of clinical experience. Inter-observer variability was assessed by the median and interquartile range of the difference between the measurements of both observers. Additionally, the L1/L4, Rad/Hum, Tib/Fem, Fib/Tib, and Hum/Fem ratios were calculated. We compared each parameter with data from previous reports of individuals with ACH as well as data from healthy controls (Langer et al., 1967; Maresh, 1955; Matsui et al., 1998; Matsui et al., 2001; Shelmerdine et al., 2016; Tsai et al., 2017).

The relationship between age and the aforementioned parameters was assessed using Spearman's rank correlation coefficient. The trend line and its formula were derived using the least-squares method. Differences between L1 and L4 in neonatal patients were evaluated using an unpaired t-test. All statistical analyses were performed using EZR version 4.0.0 (Kanda, 2013), a graphical user interface for R (The R

Foundation for Statistical Computing, Vienna, Austria). More precisely, it is a modified version of the R commander (version 2.6-2) designed to add statistical functions frequently used in biostatistics.

3 | RESULTS

Genetic analysis of *FGFR3* revealed that ACH was accompanied by the heterozygous p.Gly380Arg variant in all the patients included in this study. The number of measurements for each age and sex is presented in Table 1, whereas the number of radiographic images for each bone is shown in Supplemental Table 1. A total of 94 radiographic measurements were performed in 41 patients with ACH. There were relatively fewer data on older age and female patients, as compared to neonates and male patients, respectively.

First, the parameters Hum, Rad, Uln, Fem, Tib, Fib, L1, and L4 were measured. The mean values of each parameter according to age are presented in Supplemental Table 1. Overall, 268 bone length measurements exhibited good inter-observer agreement, with a median measurement difference of -0.01 mm (interquartile range, -0.08 to 0.05; Supplemental Figure). The length of the long bones and the interpedicular distances at L1 and L4 showed significant positive correlations with age in both sexes (Figures 2a–f and 3a, b).

The interpedicular distance becomes narrower at L4 than at L1 from childhood to adulthood in patients with ACH (Matsui et al., 1998; Matsui et al., 2001). Hence, the L1/L4 ratio and its correlation with

age were analyzed. L1 and L4 did not significantly differ during the neonatal period (L1: 0.95±0.10, L4: 0.93±0.13, p=0.50); however, L1 became wider than L4 after the neonatal period (Figure 3a, b). Consequently, the L1/L4 ratio increased with age (neonatal period: 1.03±0.08, 3 years of age: 1.16±0.12) and showed a significant positive correlation with age in both sexes (Figure 3c and Supplemental Table 2).

Because rhizomelia is a representative clinical feature of ACH, the upper segment-to-lower segment ratios in the upper and lower limbs were also analyzed. The Rad/Hum ratio (i.e., the upper-limb long bone ratio) was 0.87±0.07 during the neonatal period, indicating that the Hum was longer than the Rad during the neonatal period (Supplemental Table 2). In female patients, a significant negative correlation with age was observed. The same tendency was also identified in male patients; however, the correlation with age was not significant (Figure 4a). When both sexes were analyzed together, the Rad/Hum ratio displayed a significant negative correlation with age, suggesting that the Hum grew more than the Rad during the neonatal and infantile periods. The Tib/Fem ratio (i.e., the lower-limb long bone ratio) was 0.83±0.06 during the neonatal period (Supplemental Table 2) and did not show a correlation with age in both sexes (Figure 4b), indicating that the Fem was consistently longer than the Tib by an equal proportion during the neonatal and infantile periods.

In patients with ACH, the Fib is relatively longer than the Tib from childhood to adulthood. Accordingly, the Fib/Tib ratio was assessed to elucidate whether this is also applicable during the neonatal and infantile periods. The Fib/Tib ratio increased from 0.97±0.05 during the neonatal period to 1.05±0.05

at 3 years of age, and a significant positive correlation was observed in both sexes (Figure 4c and Supplemental Table 2).

Finally, the Hum/Fem ratio was evaluated to compare the growth of the Hum with that of the Fem. The Hum/Fem ratio was 0.88±0.07 during the neonatal period and exhibited a significant negative correlation with age in both sexes, indicating that the Fem was longer than the Hum during the neonatal period and that the Fem grew faster than the Hum (Figure 4d and Supplemental Table 2).

4 | DISCUSSION

The present study elucidated, for the first time, the radiological characteristics of skeletal development during the neonatal and infantile periods in patients with ACH accompanied by the heterozygous p.Gly380Arg variant.

No prior studies have addressed the length of upper-limb long bones in patients with ACH, as compared to the length of long bones in healthy children (Maresh, 1955). All upper-limb long bones in patients with ACH have been consistently shown to be shorter than those in healthy children from birth to 3 years of age. Arm span data obtained from patients with ACH from 2 years of age to adulthood indicated that the difference in arm span between male and female patients increased with age (Merker et al., 2018). Based on our data, forearm bones tended to grow faster in males than in females; however, no sex difference

in the growth of the humerus was found. The cause of the difference in arm span growth between males and females at 2–3 years of age may partly be attributed to the difference in forearm bone growth; nonetheless, the detailed mechanism underlying the sex difference in forearm growth remains unclear.

Langer et al. (1967) reported that the humerus in patients with ACH was short in comparison with the bones of the forearm from the neonatal period to adulthood; however, specific data were not provided. Shelmerdine et al. (2016) showed that the mean Rad/Hum ratio was significantly higher in infants with ACH (0.87 ± 0.04, n=22) in comparison with healthy controls (0.79 ± 0.04, n=150). In our study, we observed that the mean Rad/Hum ratio at 0 year of age was almost consistent with that observed in infants with ACH by Shelmerdine et al., surpassing the levels documented for healthy controls. However, we found that the Rad/Hum ratio decreased with age and, at 3 years of age, became similar to that observed in healthy infants by Shelmerdine et al. These data present a novel finding that rhizomelia in the upper limbs is a more prominent phenomenon during the neonatal period.

In addition to the upper-limb bones, our data indicated that the growth of the femur and tibia was severely impaired, as compared to that observed in healthy children (Tsai et al., 2017). This growth impairment in the lower limbs contributed to the decreased height growth during the neonatal and infantile periods (Del Pino et al., 2018; Fong et al., 2001). Previous studies reported that the Tib/Fem ratio in patients with ACH was the same as that in healthy controls from infanthood to childhood and that the lower limbs of patients with ACH did not radiologically present with rhizomelia (Langer et al., 1967; Maresh, 1955;

Shelmerdine et al., 2016). Our results are consistent with the findings of previous studies. Furthermore, our data indicated that the Tib/Fem ratio in children with ACH remained unchanged from birth to 3 years of age, suggesting that the femoral and tibial growth during this period contributed equally to lower-limb growth impairment in children with ACH.

A disproportionally long fibula compared with the tibia is a radiological characteristic observed in patients with ACH. Matsui et al. (1998) reported a mean Fib/Tib ratio of 1.12±0.03 in children with ACH from 5 to 18 years of age, which is higher than the Fib/Tib ratio of 1.04±0.05 and 1.06±0.06 found in our study for both 3-year-old males and females, respectively. Furthermore, Matsui et al. (2001) showed no significant positive correlation between age and the Fib/Tib ratio. Nehme et al. (1976) reported that the ratio of the length of the tibia to the fibula in patients with ACH began at a normal level (0.96) at age 3 and decreased with age, to approximately 0.8 at maturity. Considering these data and our results, a "disproportionally long fibula" is obscure during the neonatal period and becomes distinct with age.

A "decrease in the interpediculate distance from upper to lower lumber spine" is one of the radiological characteristics of ACH (Spranger et al., 2018). Langer et al. purported that most newborn patients with ACH have a narrower interpediculate distance at the L5 level than at the L1 level; however, occasionally at this age, the interpediculate distance is the same throughout the lumber spine. Nonetheless, specific data to substantiate this assertion was not presented (Langer et al., 1967). Our findings suggest that individuals with ACH displaying a "decrease in the interpediculate distance from

upper to lower lumber spine" are, rather, a minority among newborn patients. Two previous studies examined the L1/L4 ratio in patients with ACH with the p.Gly380Arg variant (Matsui et al., 1998; Matsui et al., 2001); however, neither of these two studies analyzed male and female patients separately. In one study assessing the L1/L4 ratio in 23 patients with ACH aged 3–17 years (Matsui et al., 1998), the mean L1/L4 ratio was 1.18±0.10, which is consistent with the data on 3-year-old males and females in our study. The other study analyzed the correlation between age and the L1/L4 ratio in 27 patients with ACH aged 3–18 years and found no correlation (Matsui et al., 2001). In our study, L1 was equal to L4 during the neonatal period. After the neonatal period, L1 and L4 showed significant positive correlations with age, and L1 became wider than L4, resulting in an increased L1/L4 ratio after the neonatal period. Considering the findings of our study and the two aforementioned previous reports, a "decrease in the interpediculate distance from upper to lower lumber spine" is not prominent during the neonatal period, and it becomes obvious to the degrees observed in adults when patients become 3 years old or older. This might reflect the earlier closure of the neurocentral synchondroses in the lower lumber spine compared to those in the upper lumber spine.

The present study has some limitations. First, we could not clarify the longitudinal trend of skeletal development in patients with ACH from childhood to adulthood because, in Japan, children with ACH receive growth hormone therapy for short stature after 3 years of age. Second, our study was conducted using retrospective data skewed toward a large number of newborns. Third, owing to the small

amount of data on long bones in the upper limbs, it remains unclear whether the difference in the Rad/Hum ratio found between males and females is truly significant. Further studies are required to resolve these issues. Despite these limitations, our study has strength in that it is the first report to analyze the radiological parameters of each bone during the neonatal and infantile periods in patients with genetically confirmed ACH and to clarify the relationship between these parameters and age by sex.

In conclusion, we radiologically characterized, for the first time, the skeletal development of patients with ACH and the heterozygous p.Gly380Arg variant of *FGFR3* during the neonatal and infantile periods. Our results suggest the need for further discussion regarding the simplistic classification of ACH as a condition characterized by rhizomelia. Recently, several therapeutic approaches to short stature in patients with ACH have been developed; C-type natriuretic peptide analogs (Lorget et al., 2012; Wendt et al., 2015; Yasoda et al., 2004) have become available for clinical use, and RNA aptamers (Kimura et al., 2021), tyrosine kinase inhibitors (Komla-Ebri et al., 2016), soluble *FGFR3* decoys (Garcia et al., 2013; Gonçalves et al., 2020), and meclizine (Matsushita et al., 2015) have been under development. We believe that our results can be used as basic data to evaluate the effectiveness of these novel therapeutic candidates for skeletal growth.

REFERENCES

Del Pino, M., Ramos Mejia, R., & Fano, V. (2018). Leg length, sitting height, and body proportions references for achondroplasia: New tools for monitoring growth. *American Journal of Medical Genetics Part A*, *176*, 896–906. *doi:*10.1002/ajmg.a.38633

Fong, D. Y., Wong, S. W., & Karlberg, J. (2001). Modelling variation of lower leg length growth in early life. *Statistics in Medicine*, *20*, 3097–3108. *doi:*10.1002/sim.921

Garcia, S., Dirat, B., Tognacci, T., Rochet, N., Mouska, X., Bonnafous, S., Patouraux, S., Tran, A., Gual, P., Le Marchand-Brustel, Y., Gennero, I., & Gouze, E. (2013). Postnatal soluble FGFR3 therapy rescues achondroplasia symptoms and restores bone growth in mice. *Science Translational Medicine*, *5*, 203ra124. *doi:*10.1126/scitranslmed.3006247

Gonçalves, D., Rignol, G., Dellugat, P., Hartmann, G., Sarrazy Garcia, S., Stavenhagen, J., Santarelli, L., Gouze, E., & Czech, C. (2020). In vitro and in vivo characterization of Recifercept, a soluble fibroblast growth factor receptor 3, as treatment for achondroplasia. *PLoS One*, *15*, e0244368. *doi:*10.1371/journal.pone.0244368

Hasegawa, K., & Tanaka, H. (2014). Children with short-limbed short stature in pediatric endocrinological services in Japan. *Pediatrics International*, *56*, 809–812. *doi:*10.1111/ped.12511

Horton, W. A., Hall, J. G., & Hecht, J. T. (2007). Achondroplasia. *The Lancet*, *370*, 162–172. *doi:*10.1016/s0140-6736(07)61090-3

Ireland, P. J., Pacey, V., Zankl, A., Edwards, P., Johnston, L. M., & Savarirayan, R. (2014). Optimal management of complications associated with achondroplasia. *The Application of Clinical Genetics*, *7*, 117–125. *doi:*10.2147/tacg.S51485

Kanda, Y. (2013). Investigation of the freely available easy-to-use software 'EZR' for medical statistics. *Bone Marrow Transplantation*, *48*, 452–458. *doi:*10.1038/bmt.2012.244

Kimura, T., Bosakova, M., Nonaka, Y., Hruba, E., Yasuda, K., Futakawa, S., Kubota, T., Fafilek, B., Gregor, T., Abraham, S. P., Gomolkova, R., Belaskova, S., Pesl, M., Csukasi, F., Duran, I., Fujiwara, M., Kavkova, M., Zikmund, T., Kaiser, J., … Krejci, P. (2021). An RNA aptamer restores defective bone growth in FGFR3-related skeletal dysplasia in mice. *Science Translational Medicine*, *13,* eaba4226. *doi:*10.1126/scitranslmed.aba4226

Komla-Ebri, D., Dambroise, E., Kramer, I., Benoist-Lasselin, C., Kaci, N., Le Gall, C., Martin, L., Busca, P., Barbault, F., Graus-Porta, D., Munnich, A., Kneissel, M., Di Rocco, F., Biosse-Duplan, M., & Legeai-Mallet, L. (2016). Tyrosine kinase inhibitor NVP-BGJ398 functionally improves FGFR3-related dwarfism in mouse model. *The Journal of Clinical Investigation*, *126*, 1871–1884. *doi:*10.1172/JCI83926

Langer, L. O., Jr., Baumann, P. A., & Gorlin, R. J. (1967). Achondroplasia. *The American Journal of Roentgenology Radium Therapy and Nuclear Medicine*, *100*, 12–26. *doi:*10.2214/ajr.100.1.12

Lorget, F., Kaci, N., Peng, J., Benoist-Lasselin, C., Mugniery, E., Oppeneer, T., Wendt, D. J., Bell, S. M.,

Bullens, S., Bunting, S., Tsuruda, L. S., O'Neill, C. A., Di Rocco, F., Munnich, A., & Legeai-Mallet, L. (2012). Evaluation of the therapeutic potential of a CNP analog in a Fgfr3 mouse model recapitulating achondroplasia. *American Journal of Human Genetics*, *91*, 1108–1114. *doi:*10.1016/j.ajhg.2012.10.014

Maresh, M. M. (1955). Linear growth of long bones of extremities from infancy through adolescence; continuing studies. *A.M.A. American Journal of Diseases of Children*, *89*, 725–742.

Matsui, Y., Kawabata, H., Ozono, K., & Yasui, N. (2001). Skeletal development of achondroplasia: analysis of genotyped patients. *Pediatrics International*, *43*, 361–363. *doi:*10.1046/j.1442-200x.2001.01416.x

Matsui, Y., Yasui, N., Kimura, T., Tsumaki, N., Kawabata, H., & Ochi, T. (1998). Genotype phenotype correlation in achondroplasia and hypochondroplasia. *The Journal of Bone and Joint Surgery. British Volume*, *80*, 1052–1056. *doi:*10.1302/0301-620x.80b6.9277

Matsushita, M., Hasegawa, S., Kitoh, H., Mori, K., Ohkawara, B., Yasoda, A., Masuda, A., Ishiguro, N., & Ohno, K. (2015). Meclozine promotes longitudinal skeletal growth in transgenic mice with achondroplasia carrying a gain-of-function mutation in the FGFR3 gene. *Endocrinology*, *156*, 548–554. *doi:*10.1210/en.2014-1914

Merker, A., Neumeyer, L., Hertel, N. T., Grigelioniene, G., Mohnike, K., & Hagenas, L. (2018). Development of body proportions in achondroplasia: Sitting height, leg length, arm span, and foot

length. *American Journal of Medical Genetics Part A*, *176*, 1819–1829. *doi:*10.1002/ajmg.a.40356

Nehme, A. M., Riseborough, E. J., & Tredwell, S. J. (1976). Skeletal growth and development of the achondroplastic dwarf. *Clinical Orthopaedics and Related Research*, *116*, 8–23.

Rousseau, F., Bonaventure, J., Legeaimallet, L., Pelet, A., Rozet, J. M., Maroteaux, P., Lemerrer, M., & Munnich, A. (1994). Mutations in the gene encoding fibroblast growth-factor receptor-3 in achondroplasia. *Nature*, *371*, 252–254. *doi:*10.1038/371252a0

Shelmerdine, S. C., Brittain, H., Arthurs, O. J., & Calder, A. D. (2016). Achondroplasia: really rhizomelic? *American Journal of Medical Genetics Part A*, *170*, 2039–2043. *doi:*10.1002/ajmg.a.37776

Shiang, R., Thompson, L. M., Zhu, Y. Z., Church, D. M., Fielder, T. J., Bocian, M., Winokur, S. T., & Wasmuth, J. J. (1994). Mutations in the transmembrane domain of FGFR3 cause the most common genetic form of dwarfism, achondroplasia. *Cell*, *78*, 335–342. *doi:*10.1016/0092-8674(94)90302-6

Spranger, J. W., Brill, P. W., Hall, C., Nishimura, G., Superti-Furga, A., Unger, S. (2018). *Bone dysplasias: an atlas of genetic disorders of skeletal development* (4th ed.). Oxford University Press.

Tsai, A., Stamoulis, C., Barber, I., & Kleinman, P. K. (2017). Infant lower extremity long bone growth rates: comparison of contemporary with early 20th century data using mixed effect models. *American Journal of Human Biology*, *29*. *doi:*10.1002/ajhb.22905

Wendt, D. J., Dvorak-Ewell, M., Bullens, S., Lorget, F., Bell, S. M., Peng, J., Castillo, S., Aoyagi-Scharber,

M., O'Neill, C. A., Krejci, P., Wilcox, W. R., Rimoin, D. L., & Bunting, S. (2015). Neutral endopeptidase-resistant C-type natriuretic peptide variant represents a new therapeutic approach for treatment of fibroblast growth factor receptor 3-related dwarfism. *The Journal of Pharmacology and Experimental Therapeutics*, *353*, 132–149. *doi:*10.1124/jpet.114.218560

Wynne-Davies, R., Walsh, W. K., & Gormley, J. (1981). Achondroplasia and hypochondroplasia. Clinical variation and spinal stenosis. *The Journal of Bone and Joint Surgery. British Volume*, *63b*, 508–515. *doi:*10.1302/0301-620x.63b4.7298674

Yasoda, A., Komatsu, Y., Chusho, H., Miyazawa, T., Ozasa, A., Miura, M., Kurihara, T., Rogi, T., Tanaka, S., Suda, M., Tamura, N., Ogawa, Y., & Nakao, K. (2004). Overexpression of CNP in chondrocytes rescues achondroplasia through a MAPK-dependent pathway. *Nature Medicine*, *10*, 80–86. *doi:*10.1038/nm971

TABLES AND FIGURES

Table 1 Numbers of measurements for each age and sex.

Ages (months)	Numbers of measurements	Male	Female
0	24 (25.5)	16 (26.7)	8 (23.5)
1 to 11	21 (22.3)	12 (20.0)	9 (26.5)
12 to 23	19 (20.2)	12 (20.0)	7 (20.6)
24 to 35	18 (19.1)	13 (21.7)	5 (14.7)
36 to 47	12 (12.8)	7 (11.7)	5 (14.7)
Total	94	60	34

Numbers within parentheses refer to the percentage of total measurements in each column.

Figure 1

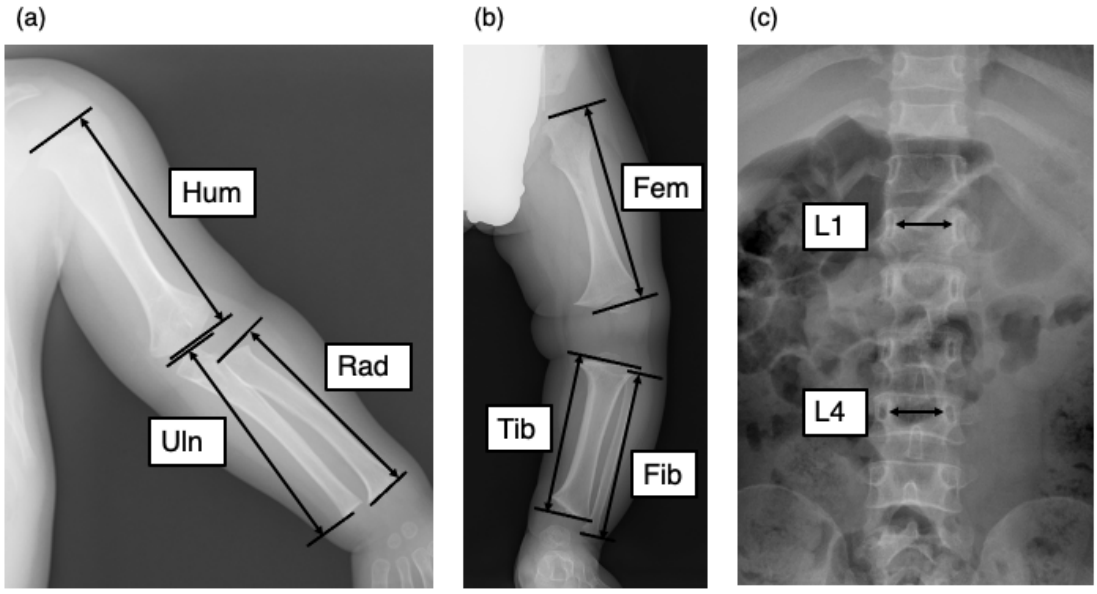

Figure 1 Radiographs showing the length of upper-limb long bones (a), the length of lower-limb long bones (b), and the interpediculate distances at L1 and L4 (c). For long bone measurements, we recorded the diaphyseal bone lengths.

Figure 2

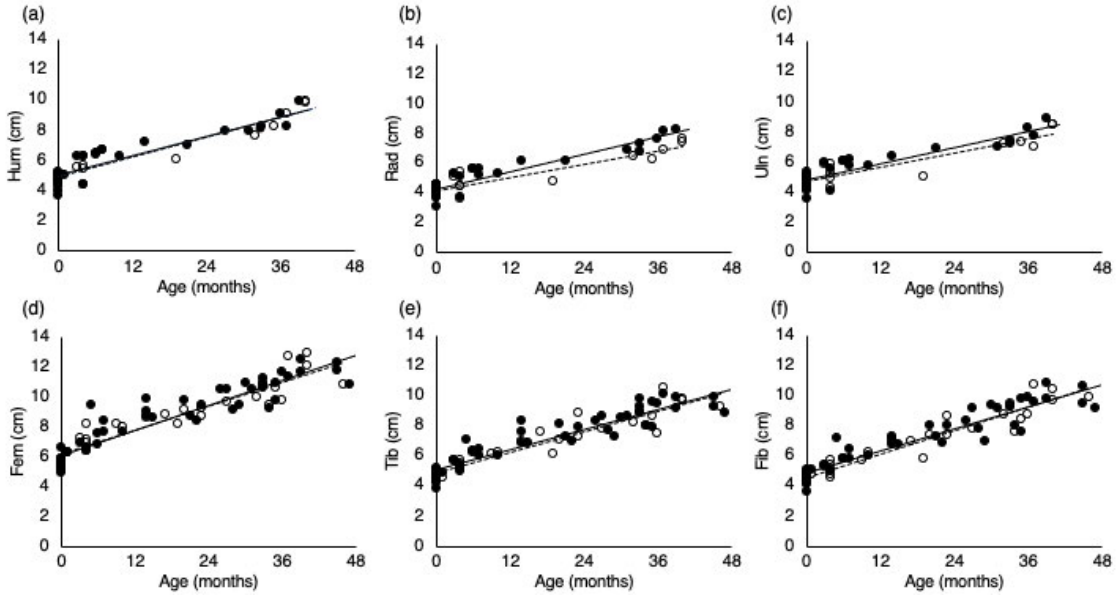

Figure 2 Relationship between age and the length of long bones (Hum, Rad, Uln, Fem, Tib and Fib). Closed and open circles represent male and female patients, respectively. When significant correlations are observed, regression lines are shown as a solid line for males and a dashed line for females. (a) Hum: male y=0.11x+5.0 (ρ=0.93, p<0.001), female y=0.11x+4.9 (ρ=0.87, p<0.001), total y=0.11x+4.9 (ρ=0.91, p<0.001). (b) Rad: male y=0.095x+4.3 (ρ=0.90, p<0.001), female y=0.075x+4.1 (ρ=0.85, p<0.001), total y=0.085x+4.3 (ρ=0.87, p<0.001). (c) Uln: male y=0.089x+4.8 (ρ=0.91, p<0.001), female y=0.080x+4.7 (ρ=0.85, p<0.001), total y=0.084x+4.8 (ρ=0.86, p<0.001). (d) Fem: male y=0.14x+6.1 (ρ=0.94, p<0.001), female y=0.13x+6.1 (ρ=0.97, p<0.001), total y=0.14x+6.1 (ρ=0.95, p<0.001). (e) Tib: male y=0.11x+5.1 (ρ=0.94, p<0.001), female y=0.11x+4.9 (ρ=0.95, p<0.001), total y=0.11x+5.0 (ρ=0.94, p<0.001). (f) Fib: male y=0.12x+4.9 (ρ=0.94, p<0.001), female y=0.13x+4.6 (ρ=0.96, p<0.001), total y=0.12x+4.8 (ρ=0.95, p<0.001). Hum, humerus; Rad, radius; Uln, ulna; Fem, femur; Tib, tibia; Fib, fibula.

Figure 3

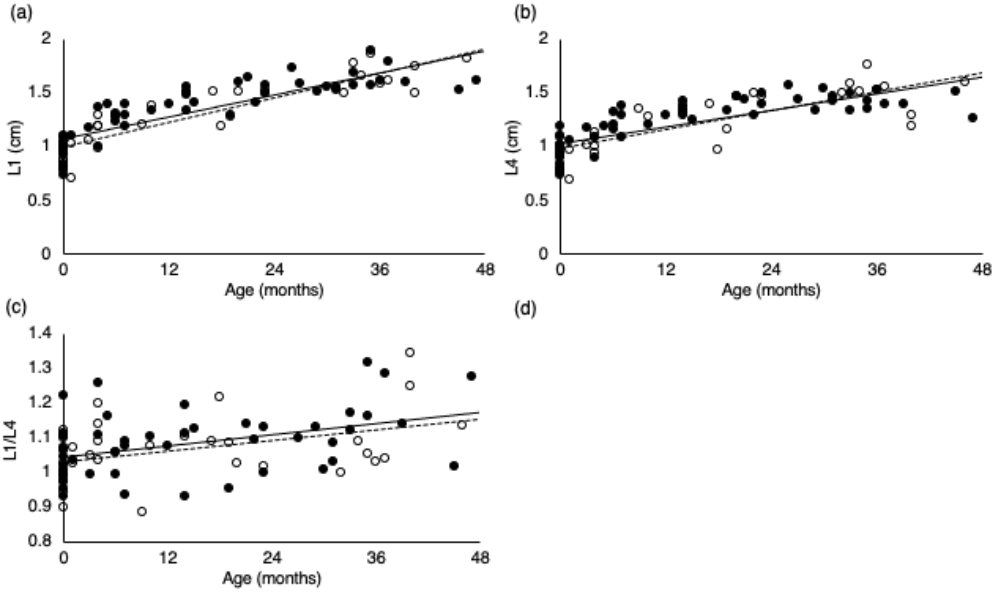

Figure 3 Relationship between age and L1, L4, and L1/L4 ratio. Closed and open circles represent male and female patients, respectively. Solid and dashed lines represent correlation diagrams of male and female patients, respectively, if significant correlations are observed. (a) L1: male y=0.017x+1.1 (ρ=0.92, p<0.001), female y=0.019x+1.0 (ρ=0.91, p<0.001), total y=0.018x+1.1 (ρ=0.92, p<0.001). (b) L4: male y=0.013x+1.0 (ρ=0.86, p<0.001), female y=0.015x+0.98 (ρ=0.83, p<0.001), total y=0.014x+1.0 (ρ=0.84, p<0.001). (c) L1/L4 ratio: male y=0.0027x+1.0 (ρ=0.45, p=0.0013), female y=0.0025x+1.0 (ρ=0.38, p=0.037), total y=0.0025x+1.0 (ρ=0.41, p<0.001).

Figure 4

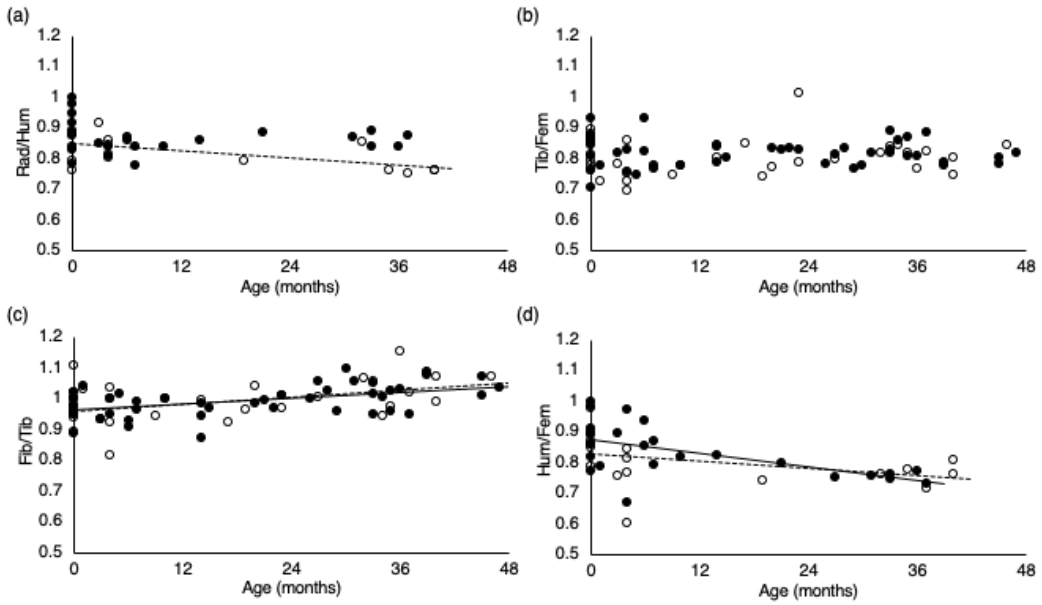

Figure 4 Relationship between age and the Rad/Hum, Tib/Fem, Fib/Tib, and Hum/Fem ratios. Closed and open circles represent male and female patients, respectively. Solid and dashed lines represent correlation diagrams of male and female patients, respectively, if significant correlations are observed. (a) Rad/Hum ratio: male (ρ=-0.075, *p*=0.73), female y=-0.0019x+0.85 (ρ=-0.61, *p*=0.012), total y=-0.0013x+0.86 (ρ=-0.34, *p*=0.031). (b) Tib/Fem ratio: male (ρ=0.067, *p*=0.66), female (ρ=0.14, *p*=0.46), total (ρ=0.046, *p*=0.70). (c) Fib/Tib ratio: male y=0.0016x+0.96 (ρ=0.48, *p*<0.001), female y=0.0019x+0.96 (ρ=0.39, *p*=0.035), total y=0.0017x+0.96 (ρ=0.43, *p*<0.001). (d) Hum/Fem ratio: male y=-0.0037x+0.87 (ρ=-0.69, *p*<0.001), female y=-0.0019x+0.83 (ρ=-0.66, *p*=0.0058), total y=-0.0029x+0.85 (ρ=-0.64, *p*<0.001). Rad, radius; Hum, humerus; Tib, tibia; Fem, femur; Fib, fibula.